

Carbon-Carbon Recuperators in Closed-Brayton-Cycle Space Power Systems

Michael J. Barrett*

NASA Glenn Research Center, Cleveland, OH, 44135

Paul K. Johnson†

Analex Corporation, Cleveland, OH, 44135

The use of carbon-carbon (C-C) recuperators in closed-Brayton-cycle space power conversion systems was assessed. Recuperator performance was forecast based on notional thermodynamic cycle state values for planetary missions. Resulting thermal performance, mass and volume for plate-fin C-C recuperators were estimated and quantitatively compared with values for conventional offset-strip-fin metallic designs. Mass savings of 40–55% were projected for C-C recuperators with effectiveness greater than 0.9 and thermal loads from 25–1400 kWt. The smaller thermal loads corresponded with lower mass savings; however, at least 50% savings were forecast for all loads above 300 kWt. System-related material challenges and compatibility issues were also discussed.

Nomenclature

A	= area
f	= Darcy friction factor
G	= heat exchanger core mass velocity
K	= resistance (pressure loss) coefficient
MW	= molecular weight (molar mass)
m	= mass
Ntu	= number of thermal units

* Research Engineer, Thermal Energy Conversion Branch, 21000 Brookpark Rd., MS 301-2, Senior Member AIAA

† Mechanical Engineer, Mechanical Systems Branch, 21000 Brookpark Rd., MS 301-2, Member AIAA

P = absolute pressure

Q = heat transfer

St = Stanton number

T = absolute temperature

ε = effectiveness

ρ = density

Subscripts

1 = flow stream one

2 = flow stream two

c = contraction

cr = core

e = expansion

Superscripts

$'$ = time rate of change

I. Introduction

Carbon-carbon (C-C) material is used in many engineering applications because of its high thermal conductivity, elevated temperature capability and low density. Closed-Brayton-cycle (CBC) space power conversion systems (PCS) will need compact heat exchangers with all of these attributes¹. Excluding the heat rejection system radiator, the recuperator is often the heaviest component in a CBC PCS. In many low-pressure-ratio cycles, the recuperator can reduce entropy generation and increase cycle efficiency by transferring thermal energy between hot and cold portions of the cycle. The role of recuperative heat transfer is illustrated in Fig. 1. Because enhanced recuperator performance could increase efficiency or save mass in CBC systems, applied study of C-C heat exchangers is warranted. Potential advantages and challenges of C-C heat exchangers can be found in the literature; some examples follow.

Stevenson et al.² studied a compact heat exchanger with a C-C core as a replacement for the F/A-18E/F nickel-based-alloy primary heat exchanger. Dimensions of the C-C and metallic cross-flow heat exchangers were the same. The metal core used offset strip fins; manufacturing capabilities limited the C-C core to continuous (plain)

fins. The C-C design had a predicted weight savings of 40% with performance that met or exceeded the metal heat exchanger.

Alam et al.³ experimentally determined friction and Colburn factors for a single layer of a C-C plate-fin (24 fins per inch) heat exchanger. Compared to a Kays and London plate-fin configuration with approximately 20 fins per inch, the C-C single layer data exhibited lower values for both factors. However, high C-C thermal conductivity resulted in improved total surface temperature effectiveness over metal heat exchangers.

Kearns et al.⁴ evaluated brazing techniques used to construct a C-C compact heat exchanger core. Inconsistent fin heights caused the parting plate to bond to the taller but not the shorter fins. Their experiments demonstrated the necessity of tightly controlled fabrication processes to ensure more uniform fin heights. Another height-related problem occurred when parting plates were joined. Because the plates were not perfectly flat, only the high points bonded. They concluded that instead of brazing the fins to the plate, a preferred alternative is to manufacture an integral design that co-processes the fins with top and bottom parting plates as one piece, thereby requiring braze joints only between parting plates.

Watts et al.⁵ examined stacked layers of integral C-C surfaces. The fin-to-plate joints displayed excellent carbon bonds and the plate-to-plate joints showed good braze bonds. A thickly applied braze material between the plates reduced the problem of only high points bonding.

Not all joints in a C-C heat exchanger will be between like materials; for practical application, C-C and metal interfaces must exist. Kennel and Deutchman⁶ described a technique that used an ion beam to deposit a metallic interface material at shallow depths into the surface of each material. With the surfaces treated, they could be joined together using a metal-to-metal bonding technique. Dissimilar materials can also be joined using a braze. In 2004, Materials Resources International⁷ advertised an active braze method to join C-C with metal and withstand temperatures up to 2000 °C.

In addition to potential advantages, from the literature we glean that technology associated with C-C heat exchangers has progressed to a level where meaningful component studies can occur. The present work assesses C-C recuperators in CBC systems for space power applications. First, a series of CBC state point cases are defined. After describing a conventional heat exchanger design code, several concept recuperators are designed for each of the defined cases. Conventional metallic designs are contrasted with C-C constructions; mass and volume comparisons are made. Other integration issues are briefly addressed and conclusions are presented.

II. Evaluation Method

Thermodynamic state points were determined for nine notional CBC power conversion systems with power outputs ranging from 2 – 300 kWe. Associated recuperator thermal loads varied from 24 – 1380 kWt with effectiveness values greater than 0.9. A state point example for a 300-kWe case is shown in Fig. 2. For each power conversion case identified, conceptual designs were created for six conventional metallic recuperators and for two C-C recuperators with the same thermal-fluid performance (thermal load and pressure drop were matched for all designs). The six conventional designs were generated using three different plate-fin geometries and two different metals. The C-C designs shared a plate-fin geometry (slightly simpler than the metallic exchangers) but used different fiber-based materials of construction. Mass and volume characteristics of the eight designs were compared.

A. Case Definition

The nine power conversion cases are defined in Table 1. The CBC working fluid is a mixture of Helium and Xenon in all cases; molecular weight (MW) for each case is given. Bulk temperatures and pressures are specified. The first two cases (2 and 10.5 kWe) represent CBC conversion systems that were actually fabricated. The 10.5-kWe system was called the Brayton Rotating Unit (BRU)⁸ and was configured with an integrated stainless steel recuperator and gas-cooler called the Brayton Heat Exchanger Unit (BHXU)⁹. The counterflow recuperator in the BHXU used plate-fin construction similar to that modeled in the present study. The Hastelloy-X recuperator in the 2-kWe mini-Brayton-Rotating-Unit (miniBRU) system¹⁰ was a plate-fin, counterflow heat exchanger using offset fins in the core and plain fins in transition areas. The BRU and miniBRU hardware will be used to gauge the baseline accuracy of the heat exchanger conceptual design code.

B. Heat Exchanger Conceptual Design

Conceptual designs for balanced counterflow recuperators were generated using a NASA conceptual design code called HXCALC. (Balanced conditions are often assumed during conceptual design of CBC recuperators; designs are later refined to include compressor bleed flow imbalances.) The code uses a conventional design algorithm¹¹ to roughly size the heat exchanger based on thermal requirements then adjusts the design to meet pressure-drop constraints.

State point information and fluid properties are provided as input so that an initial guess of core mass velocity, G , can be made,

$$G \approx 2(\Delta P \rho_{mean} St / f Ntu)^{0.5} \quad (1)$$

Equation (1) uses the balanced flow assumption to replace the one-sided Ntu_1 with the overall Ntu , $Ntu_1 = 2 Ntu$. An apparent factor of 4 difference between Eq. (1) and the expression used by Kays and London¹¹ is due only to the difference between the Darcy and Fanning friction factors, $f_{\text{Fanning}} = f/4$. Geometry-specific heat transfer correlations, $St = \text{fn}(Re, Pr)$, and fin efficiencies are used to determine the overall heat transfer coefficient and required heat transfer area. The required area sets the recuperator length. Corresponding correlations for f are used so that pressure-drop through the exchanger can be calculated,

$$\Delta P/P_1 = \frac{G^2}{2\rho_1 P_1} \left[(K_c + 1 - \sigma^2) + 2 \left(\frac{\rho_1}{\rho_2} - 1 \right) + \frac{fA\rho_1}{4A_{cr}\rho_{mean}} - (1 - \sigma^2 - K_e) \frac{\rho_1}{\rho_2} \right] \quad (2)$$

and a new mass velocity is estimated. These calculations proceed in an iterative loop until thermal load and pressure-drop requirements are satisfied. The final geometry is then used to estimate the recuperator mass. The mass estimate includes contributions from side- and end-walls that are used for pressure-vessel containment of heat exchanger entrance, core and exit regions. The side- and end-walls are metallic in all designs (including those with C-C cores). Wall thicknesses are based on an as-built reference design configuration and scaled linearly with mean operating pressure.

Use of carbon-carbon material in conceptual design influences three principle factors in the calculations: plate-fin geometries, thermal conductivity and density.[‡] Offset strip fins were selected for metallic core designs; however, plain fins were used to ease manufacture with C-C sheeting. Also, plate thicknesses for C-C configurations were increased to 0.635 mm from the metallic value of 0.203 mm. The C-C plate and fin selections used in this study are representative of state-of-the-art manufacturing capabilities¹². Widely accepted conductivity and density values for stainless steels and Hastelloy X are available in the reference literature. However, significant variations in C-C properties do exist; ply configuration and processing for C-C sheets strongly affects in-plane and through-plane conductivity values. Two sets of values were chosen for this study – one for high-performance (HP) sheeting and one for low-performance (LP). In-plane conductivity of 260 W/m-K and through-plane of 15 W/m-K represented the high-performance set. Low-performance (and lower cost) sheeting was assumed to have in-plane and through-plane values of 150 W/m-K and 10 W/m-K, respectively. Fiber orientation could be used to preferentially reduce

[‡] Surface roughness variation was neglected.

stream-wise conduction in fins and thereby increase thermal performance; however, 2-D in-plane isotropy was assumed in the present work. A density of 1800 kg/m³ was used for both HP and LP sheets.

III. Results and Discussion

Detailed results from the design cases are given in Table 2. Fin configurations are identified using the reference terminology of Kays and London¹¹. As expected, the stainless steel designs outperform the Hastelloy X designs (less mass and volume) in all like-finned cases. In practice, Hastelloy X is sometimes chosen over stainless steel to maintain structural integrity when exchanger duty is expected to include many high-thermal-stress temperature cycles.

The “as-built” reference data of the miniBRU and BRU recuperators are included as footnotes in the table to illustrate the degree of agreement between the heat exchanger conceptual design code and actual hardware. The as-built fin configurations differ from the general fin geometries available in the code, so a representative high-performance fin design is chosen for comparison. Many heat transfer correlations can be expected to carry $\pm 20\%$ uncertainty over the applicable correlation range. The uncertainty may increase for low-Re flows in low-Pr mixtures of He and Xe¹³. Consequently, considering geometry differences and correlation uncertainties, the miniBRU and BRU core mass discrepancies of 18% and 15% are not surprising. Also, the HXCALC conceptual design code neglects heat transfer in the inlet and exit transition regions; the core is sized to provide all of the necessary heat transfer. In actuality, a significant percentage of the heat transfer can occur in the transitions; high-fidelity exchanger design and CBC codes account for this effect¹⁴. Additional sources of error are numerous; flow nonuniformity, manufacturing tolerances and variations in design safety factors are just a few examples. As a result, $\pm 25\%$ uncertainty is carried on mass predictions in this work.

In all cases, recuperators made with C-C cores were predicted to have significantly lower masses than the minimum mass metallic exchanger. Figure 3 shows the ratio of the C-C LP mass to the minimum metallic mass for each case; this ratio is termed the “relative mass” (with respect to the lightest metallic exchanger). Even with the propagated 35% uncertainty, the potential mass savings is evident. For loads greater than 300 kWt, the C-C LP exchanger is forecast to weigh at least 50% less than the lightest metallic exchanger.

Relative volumes of the C-C LP exchanger designs are shown in Fig. 4. (Since uncertainty in mass is directly related to the projected heat transfer area, similar uncertainty is present in the volume estimate.) Most designs show approximately 50% more volume is needed for the C-C LP design relative to the smallest metallic exchanger. The

primary reason for this is the choice of plain fins in the C-C geometry. Because plain fins generally have lower average convective heat transfer coefficients compared to strip fins, despite the increased C-C fin efficiencies, the plain fins still require more surface area to provide the same performance. At the lowest loads (lowest-Re cases), nearly twice as much volume is required for the C-C LP exchanger. Since mass advantage diminishes at lower thermal loads, if plain fins are required to ease C-C construction, the combination of mass and volume trends suggests that C-C exchangers may be advantageous only for loads above 300 kWt; loads greater than 300 kWt can be achieved in C-C cores with approximately 55% mass savings and a 50% volume penalty. However, if strip fins can be used in C-C construction, the trends change. For example, if strip fins are used in a C-C core for the miniBRU case, the C-C LP volume drastically reduces from 180% to 84% of the minimum metallic exchanger. (The associated relative mass reduces from 58% to 30% of the minimum.) Developing manufacturing technology that enables reliable strip-fin C-C core construction may yield major benefits to CBC system designs.

IV. Other CBC Integration Issues

Because of the aforementioned potential benefits, C-C recuperator cores should be considered in CBC system designs. However, there are system-level integration risks that, unless adequately mitigated, prohibit prudent adoption of C-C designs in CBC flow loops. By introducing C-C components, the very low coefficient of thermal expansion (CTE) of a C-C element must not induce unacceptable stresses in other components or interfaces with higher CTE values. Creatively designed cores and interfaces must be investigated to alleviate the CTE-mismatch problem. Joining C-C elements to one other or to metallic components in the system also raises another concern. Despite previous contributions and ongoing development work¹⁵, brazing C-C parts is still a relatively immature technology; high-temperature joint reliability and lifetime is unproven for C-C and carbon-to-metal joints in CBC-type service environments. Additionally, long-term compatibility of C-C surfaces in CBC flow passages must be scrutinized. Because of the contamination sensitivity of refractory metal alloys likely to be used in heat-source heat exchangers (HSHX)¹⁶, surface transport of carbon into the working fluid may yield concentrations of C or CO₂ (if combined with oxygen from superalloy components) that are unacceptable for long-life mission requirements. Additional research is needed to adequately assess these issues.

V. Conclusions

High thermal conductivity, elevated temperature capability and low density make carbon-carbon material an interesting candidate for fabrication of high-performance recuperators in closed-Brayton-cycle space power

conversion systems. Mass savings of 40–55% were projected for carbon-carbon recuperators with effectiveness greater than 0.9 and thermal loads from 25–1400 kWt. At loads greater than 300 kWt, the carbon-carbon exchanger was consistently predicted to weigh at least 50% less than the lightest metallic exchanger.

When carbon-carbon fin geometry was limited to plain fins (for ease of fabrication), most lower-performance carbon-carbon material designs showed approximately 50% more volume was needed relative to the smallest metallic exchanger. When plain fins are used, carbon-carbon exchangers are most attractive at loads greater than 300 kWt.

When strip fins were allowed in the carbon-carbon designs, a 24-kWt exchanger volume reduced from 180% to 84% of the minimum equivalent metallic exchanger. The associated relative mass reduced from 58% to 30% of the minimum. Therefore, developing manufacturing technology to enable construction of carbon-carbon strip fin cores will expand the useful range of applicability for carbon-carbon recuperators.

Finally, there are integration risks that must be mitigated before carbon-carbon designs are utilized in CBC flow loops. Brazing complications, CTE-mismatch and chemical compatibility issues must be resolved to produce reliable hardware for long-life mission scenarios.

Acknowledgments

NASA's Prometheus Nuclear Systems Program supported the work described within this paper, in whole or part, as part of the program's technology development and evaluation activities. Any opinions expressed are those of the authors and do not necessarily reflect the views of NASA, the Department of Energy, or the Prometheus Nuclear Systems Program. The authors thank Mr. Andrew G. Naples for his independent analyses of heat exchanger mass and volume estimates.

References

¹Barrett, M. J., "Expectations of Closed-Brayton-Cycle Heat Exchangers in Space Power Systems," *Journal of Propulsion and Power*, Vol. 21, No. 1, 2005, pp. 152-157.

²Stevenson, R. D., Vrable, D. L., and Watts, R. J., "Development of an Intermediate Temperature Carbon-carbon Heat Exchanger for Aircraft Applications," *Proceedings of the 44th International SAMPE Symposium*, Vol. 44, No. 2, Society for the Advancement of Material and Process Engineering, Covina, 1999, pp. 1888-1897.

³Alam, M.K., Watts, R.J., and Price, J., "Compact Carbon-Carbon Composite Heat Exchanger," *Proceedings of ASME International Mechanical Engineering Congress & Exposition*, Vol. 372, No. 4, American Society of Mechanical Engineers, New York, 2002, pp. 31-38.

⁴Kearns, K. M., Anderson, D. P., and Watts, R., "Brazing of Carbon-carbon for An Aircraft Heat Exchanger," *Proceedings of the 44th International SAMPE Symposium*, Vol. 44, No. 2, Society for the Advancement of Material and Process Engineering, Covina, 1999, pp. 1898-1908.

⁵Watts, R.J., Price, J., Daniels, D., Vrable, D., and Klosterman, E., "Joint Attachment of Carbon-Carbon Aircraft HX Core," *Proceedings of 46th International SAMPE Symposium*, Vol. 46, No. 1, Society for the Advancement of Material and Process Engineering, Covina, 2001, pp. 658-670.

⁶Kennel, E.B., and Deutchman, A.H., "Joining Carbon Composite Fins to Metal Heat Pipes Using Ion Beam Techniques," *Proceedings of the Intersociety Energy Conversion Engineering Conference*, Vol. 2, Society of Automotive Engineers, Warrendale, 1992, pp. 323-328.

⁷"WideGap™ Joining Solutions," *Materials Resources International* [online], URL: <http://www.materialsresources.com/apps/widegap.htm> [cited 06 May 2004].

⁸Davis, J. E., "Design and Fabrication of the Brayton Rotating Unit," NASA CR-1870, March 1972.

⁹Morse, C. J., Richard, C. E., and Duncan J. D., "Brayton Heat Exchanger Unit Development Program," NASA CR-120816, May 1971.

¹⁰Killackey, J. J., Graves, R., and Mosinskis, G., "Design and Fabrication of the Mini-Brayton Recuperator (MBR)," NASA CR-159429, April 1978.

¹¹Kays, W. M., and London, A. L., *Compact Heat Exchangers*, 2nd ed., McGraw-Hill, New York, 1964, p. 701.

¹²Vrable, D. L., and Shih, W., "Experimental Measurements of Heat Transfer and Pressure Drop Characteristics for Carbon Foams," *26th Annual Conference on Composites, Materials and Structures*, Cocoa Beach, FL, 2002.

¹³Taylor, M. F., Bauer, K. E., and McEligot, D. M., "Internal forced convection to low-Prandtl-number gas mixtures," *Int. J. Heat Mass Transfer*, Vol. 31, No. 1, 1988, pp. 13-25.

¹⁴Klann, J.L., "Closed Cycle Engine Program Operational Manual," NASA Lewis Research Center, Cleveland, Ohio, April 1991.

¹⁵Singh, M., Shpargel, T. P., Morscher, G., and Asthana, R., "Active metal brazing and characterization of brazed joints in titanium to carbon-carbon composites," *Proceedings of the 5th International Conference on High Temperature Ceramic Matrix Composites*, Wiley, Hoboken, 2005, pp. 457-562.

¹⁶Bowman, C., and Ritzert, F., "Compatibility of Superalloys in a Flowing He-Xe Power Conversion/Reactor System," *Proceedings of the 2nd International Energy Conversion Engineering Conference*, Vol. 3, AIAA, Washington, DC, 2004, pp. 1592-1598.

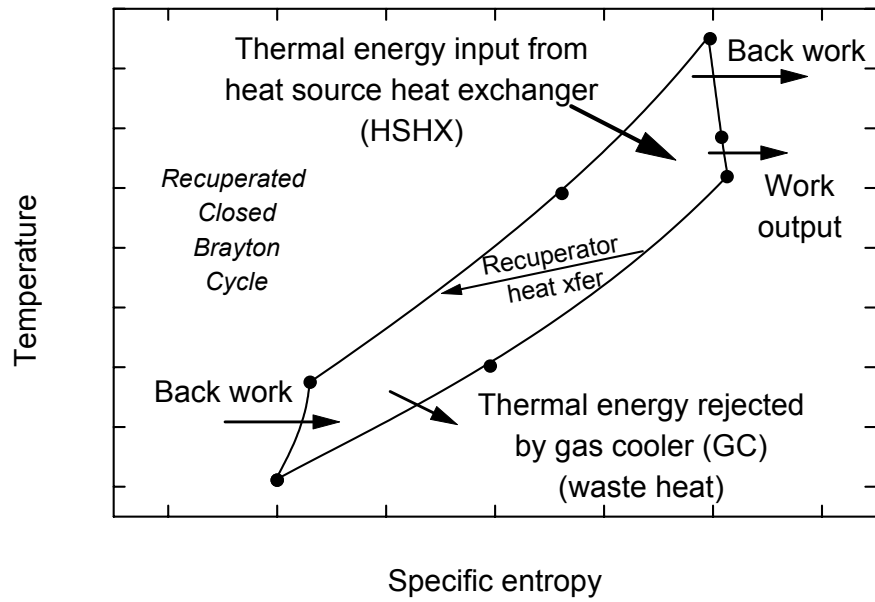


Fig. 1. Closed-Brayton-Cycle T-s Diagram.

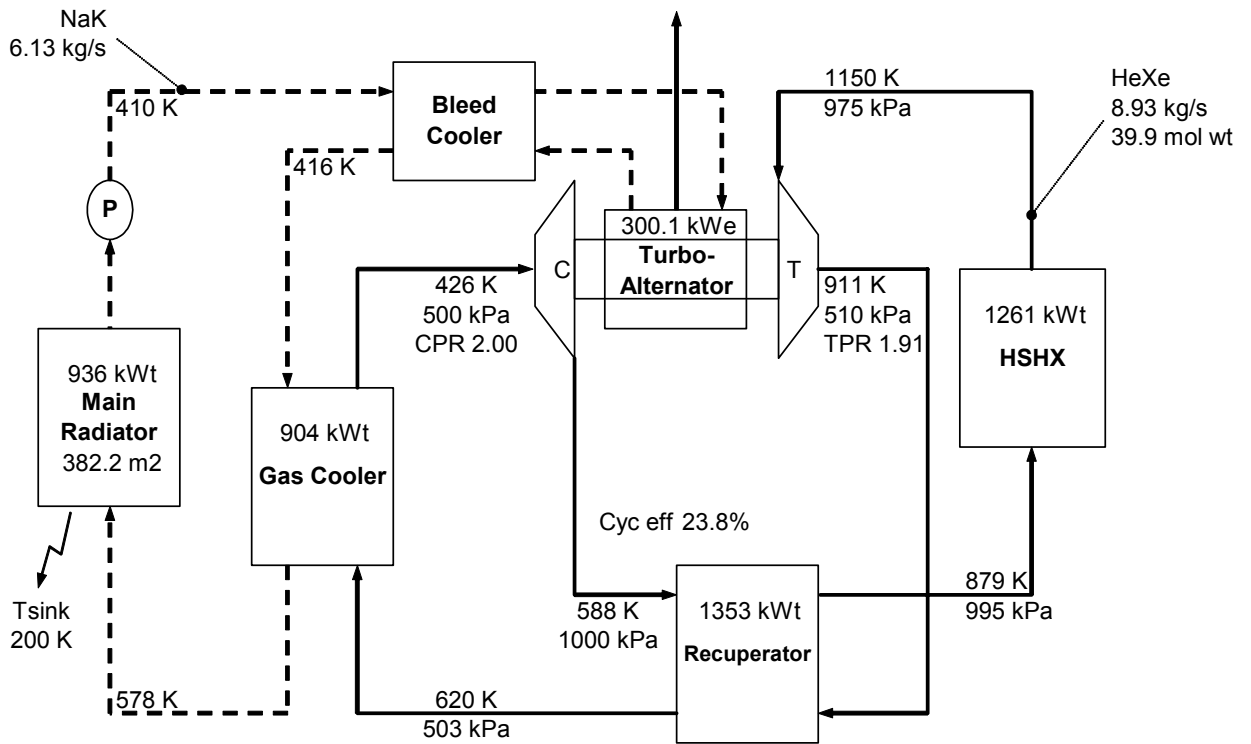


Fig. 2. Example state points for a 300-kWe PCS.

Table 1. Cases examined.

Case #	Power (kWe)	Q' (kWt)	m' (kg/s)	MW	ϵ	(DP/P)tot	Hot Stream				Cold Stream			
							Tin	Tout	Pin	Pout	Tin	Tout	Pin	Pout
1	2*	24	0.16	83.8	0.98	0.7%	995	395	494	491.6	380	980	732	730.4
2	10**	168	0.58	83.8	0.95	3.5%	944	437	170	166.5	410	917	311	306.7
3	55	261	1.72	39.9	0.9	1.9%	911	620	510	503	588	879	1000	995
4	55	272	1.77	39.9	0.92	1.9%	911	616	510	503	590	885	1000	995
5	105	619	3.85	39.9	0.92	2.0%	914	601	710	700	573	886	1373	1365
6	105	665	3.91	39.9	0.95	2.9%	919	592	710	700	575	902	1380	1360
7	200	927	5.99	39.9	0.92	1.9%	911	614	510	503	588	885	1000	995
8	300	1353	8.93	39.9	0.9	1.9%	911	620	510	503	588	879	1000	995
9	300	1380	8.91	39.9	0.92	1.9%	911	614	510	503	588	885	1000	995

*MiniBRU (1978)

**BRU (1972)

All temperatures in K; all pressures in kPa

Table 2. Conceptual design results.

Case #	Material	Fin Configuration	Core (kg)	Total (kg)	Vol (m ³)
1	Hast-X	Strip-fin plate-fin surface 1/8-15.2	61	114	0.066
		Strip-fin plate-fin surface 3/32-12.22	51	126	0.097
		Strip-fin plate-fin surface -16.00(D)	40*	64*	0.026*
	SS304	Strip-fin plate-fin surface 1/8-15.2	56	105	0.062
		Strip-fin plate-fin surface 3/32-12.22	47	115	0.090
		Strip-fin plate-fin surface -16.00(D)	37	60	0.025
	C-C HP	Plain plate-fin surface 19.86	18	36	0.046
C-C LP	Plain plate-fin surface 19.86	18	37	0.047	
2	Hast-X	Strip-fin plate-fin surface 1/8-15.2	105	127	0.114
		Strip-fin plate-fin surface 3/32-12.22	88	119	0.166
		Strip-fin plate-fin surface -16.00(D)	68	79	0.045
	SS304	Strip-fin plate-fin surface 1/8-15.2	96	116	0.106
		Strip-fin plate-fin surface 3/32-12.22	80	108	0.154
		Strip-fin plate-fin surface -16.00(D)	64**	74**	0.043**
	C-C HP	Plain plate-fin surface 19.86	31	39	0.079
C-C LP	Plain plate-fin surface 19.86	31	39	0.080	
3	Hast-X	Strip-fin plate-fin surface 1/8-15.2	120	191	0.130
		Strip-fin plate-fin surface 3/32-12.22	109	212	0.205
		Strip-fin plate-fin surface -16.00(D)	84	122	0.055
	SS304	Strip-fin plate-fin surface 1/8-15.2	109	175	0.121
		Strip-fin plate-fin surface 3/32-12.22	100	197	0.193
		Strip-fin plate-fin surface -16.00(D)	77	112	0.051
	C-C HP	Plain plate-fin surface 19.86	29	52	0.075
C-C LP	Plain plate-fin surface 19.86	31	54	0.079	
4	Hast-X	Strip-fin plate-fin surface 1/8-15.2	162	251	0.176
		Strip-fin plate-fin surface 3/32-12.22	146	274	0.275
		Strip-fin plate-fin surface -16.00(D)	112	158	0.073
	SS304	Strip-fin plate-fin surface 1/8-15.2	148	230	0.164
		Strip-fin plate-fin surface 3/32-12.22	134	254	0.259
		Strip-fin plate-fin surface -16.00(D)	103	146	0.069
	C-C HP	Plain plate-fin surface 19.86	41	69	0.104
C-C LP	Plain plate-fin surface 19.86	43	72	0.109	
5	Hast-X	Strip-fin plate-fin surface 1/8-15.2	293	470	0.318
		Strip-fin plate-fin surface 3/32-12.22	274	538	0.515
		Strip-fin plate-fin surface -16.00(D)	211	307	0.138
	SS304	Strip-fin plate-fin surface 1/8-15.2	267	432	0.296
		Strip-fin plate-fin surface 3/32-12.22	252	499	0.485
		Strip-fin plate-fin surface -16.00(D)	193	283	0.129
	C-C HP	Plain plate-fin surface 19.86	67	120	0.170
C-C LP	Plain plate-fin surface 19.86	72	128	0.183	
6	Hast-X	Strip-fin plate-fin surface 1/8-15.2	582	879	0.631
		Strip-fin plate-fin surface 3/32-12.22	529	968	0.996
		Strip-fin plate-fin surface -16.00(D)	407	561	0.266
	SS304	Strip-fin plate-fin surface 1/8-15.2	529	804	0.588
		Strip-fin plate-fin surface 3/32-12.22	486	895	0.937
		Strip-fin plate-fin surface -16.00(D)	373	517	0.250
	C-C HP	Plain plate-fin surface 19.86	144	238	0.366
C-C LP	Plain plate-fin surface 19.86	152	251	0.389	
7	Hast-X	Strip-fin plate-fin surface 1/8-15.2	554	740	0.601
		Strip-fin plate-fin surface 3/32-12.22	499	759	0.938
		Strip-fin plate-fin surface -16.00(D)	382	486	0.250
	SS304	Strip-fin plate-fin surface 1/8-15.2	504	677	0.560
		Strip-fin plate-fin surface 3/32-12.22	458	702	0.883
		Strip-fin plate-fin surface -16.00(D)	351	448	0.235
	C-C HP	Plain plate-fin surface 19.86	139	197	0.353
C-C LP	Plain plate-fin surface 19.86	146	206	0.371	
8	Hast-X	Strip-fin plate-fin surface 1/8-15.2	621	820	0.674
		Strip-fin plate-fin surface 3/32-12.22	567	841	1.066
		Strip-fin plate-fin surface -16.00(D)	435	550	0.285
	SS304	Strip-fin plate-fin surface 1/8-15.2	565	750	0.628
		Strip-fin plate-fin surface 3/32-12.22	521	777	1.003
		Strip-fin plate-fin surface -16.00(D)	399	507	0.267
	C-C HP	Plain plate-fin surface 19.86	152	213	0.388
C-C LP	Plain plate-fin surface 19.86	162	225	0.412	
9	Hast-X	Strip-fin plate-fin surface 1/8-15.2	824	1065	0.894
		Strip-fin plate-fin surface 3/32-12.22	742	1074	1.396
		Strip-fin plate-fin surface -16.00(D)	569	705	0.372
	SS304	Strip-fin plate-fin surface 1/8-15.2	749	973	0.833
		Strip-fin plate-fin surface 3/32-12.22	681	992	1.313
		Strip-fin plate-fin surface -16.00(D)	522	650	0.350
	C-C HP	Plain plate-fin surface 19.86	206	281	0.525
C-C LP	Plain plate-fin surface 19.86	217	294	0.552	

* MiniBRU (1978): 0.023 m³; 34 kg core; 59 kg total

** BRU (1972): 75 kg core; total n/a (BHXU)

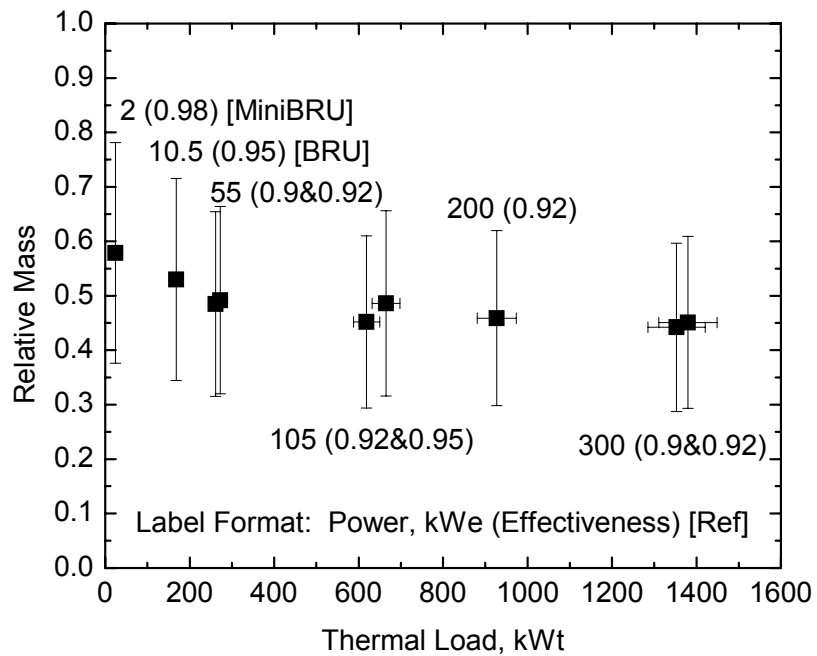


Fig 3. Relative mass of recuperator with low performance, plain-fin C-C core.

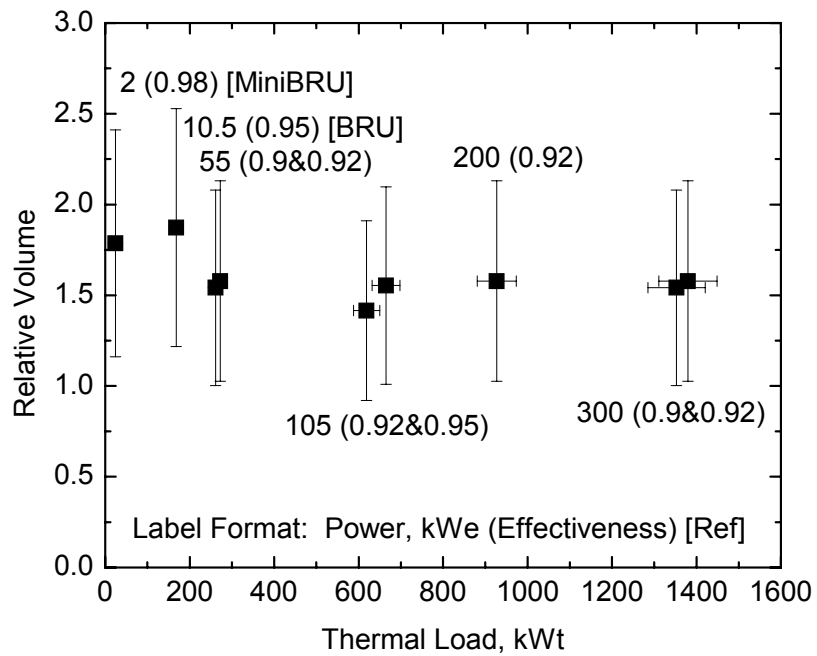


Fig. 4. Relative volume of recuperator with low-performance, plain-fin C-C core.